https://doi.org/10.1016/j.nanoen.2020.105373

Organogel Electrode Enables Highly Transparent and Stretchable Triboelectric Nanogenerators of High Power Density for Robust and Reliable Energy Harvesting

Titao Jing, Bingang Xu,* Yujue Yang, Meiqi Li, Yuanyuan Gao

Nanotechnology Center, Institute of Textiles and Clothing, The Hong Kong

Polytechnic University, Hung Hom, Kowloon 999077, Hong Kong

* Corresponding author, E-mail: tcxubg@polyu.edu.hk

Abstract

Rapid advancements in stretchable and multifunctional next-generation electronics have raised great demand in development of transparent, stretchable and reliable power sources. Here, an organogel electrode, consisted of Poly(4-acryloylmorpholine) frame and low polarity propylene carbonate swelling solvent, was prepared for constructing a new kind of organogel ionic electrode based triboelectric nanogenerator (TENG), called Og-TENG, which not only possessed high transparence (95%) and stretchability (~387%), but also exhibited excellent electric reliability and mechanical robustness (foldable and twistable) under daily working temperature range (-20℃- 45℃). The electric performance of Og-TENG is extraordinary, reaching a high instantaneous power density of 4.03 W/m^2. The rational design of organogel electrode endowed the Og-TENG with excellent anti-freezing and solvent retention properties. Moreover, the good compatibility between organogel and triboelectric elastomer improved the interface adhesion and further made Og-TENG as a high reliable device under mechanical deformations as compared to high polarity gels based TENGs. The Og-TENG was demonstrated in harvesting bio-mechanical energies and detecting human gestures. This work provides a new strategy to prepare transparent and stretchable TENGs of high power density for reliable and robust energy harvesting in daily working temperature range, exhibiting promising potentials in development of stretchable and multifunctional next-generation electronics.

Keywords: Organogel; Ionic electrode; Reliable triboelectric nanogenerator; Propylene carbonate

1.Introduction

The rapid growth of next-generation portable electronics has aroused immense enthusiasm in development of transparent, flexible and deformable devices which could not be achieved by present rigid electronics.[1-4] The application scenarios of next-generation portable electronics are various in human lives, from tactile sensors, electronic skins, soft robotics to optoelectronic devices, etc.[5-19] The advantages of flexibility and deformability are preferred in intimate integration with the human body, which would not weaken the electronics' performance.[20, 21] However, the electricity supply of such devices emerged as a big challenge as the corresponding transparency, flexibility and deformability are also the requirements of self-charging power sources, which could not be met by traditional power sources.[21-24]

Triboelectric nanogenerator (TENG) has arrested great attention as it has been proved to be a promising next-generation power source of many advantages, such as vast material choice, light weight, simple structure, and high conversion efficiency.[2, 20, 25-27] The working principle of TENG is based on the coupling of triboelectric effect and electrostatic induction. Since 2012, TENG has been widely explored for broad application scenarios, such as mechanical vibration and bio-mechanical energy harvesting, wind and water waves energy harvesting.[5, 26, 28-30] The power density of TENG is sufficient to drive many small electronics towards the new era of self-powered electronics.[27] Generally, TENG is composed of two separated dissimilar materials with distinct charge affinities and corresponding back electrodes.[27, 31]

However, currently used TENG's back electrodes are generally metallic such as Al/Cu sheet which are not suitable for transparent and stretchable TENG devices. To address the challenge, several transparent and stretchable electrodes have been developed, such as metallic conductors embedded stretchable matrix and hydrogel ionic conductors.[3] Among them, gel based electrodes are more attractive because of their softness, high stretchability, and transparency in visible region.[25, 32, 33] These gels are usually composed of three-dimensional (3D) polymer as network and corresponding liquid ionic conductors such as inorganic salts water solution, ionic liquids.[3, 25, 32]

Up to now, hydrogels or ionongels have been explored for their applications in gel based electrodes as the gels' advantages in aforementioned paragraph. However, hydrogels fall significantly short of in real applications because of two major concerns.[32-35] One is the gels' embrittlement problem at low temperature due to the high freezing point of water, which induces the loss of gels' softness and stretchability. The other concern of hydrogels is the dehydration along with time because of the water's low boiling point, which induces the solvent evaporation at high temperature in long time and further loss of gels' softness, stretchability and even conductivity.[32, 33, 35] To address the problem of hydrogels, some researchers such as Lijie Sun and Gengrui Zhao presented ionogels were due to the wide temperature range between freezing point and boiling point of ionic liquids used in ionogels.[32, 33, 36] Nevertheless, low compatibility between high polarity gels conductor and low polarity triboelectric elastomer usually induces weak adhesion in the interface.[37-39] Consequently, the mechanical reliability of high polarity gel electrode based TENG is

a critical challenge due to the delamination of high polarity gel electrode and low polarity triboelectric elastomer upon mechanical deformation.[37] Some works from Ting Liu and Younghoon Lee proposed chemical bonding between electrode layer and triboelectric elastomer layer to boost the toughness of interface by the surface chemical modification of triboelectric elastomer.[37-39] However, the complex process of preparation and less transparency of assembled TENG blocked chemical bonding's advantages.[20, 39]

Here, an organogel ionic conductor was presented in this work for designing and fabricating highly transparent, soft and robust TENG electrodes as well as TENG devices on the purpose of addressing the challenges mentioned above. The swelling solvent of organogel was selected as propylene carbonate (PC) because its large temperature range between freezing point of -49 ℃ and boiling point of 242 ℃, good chemical stability, low vapor pressure, and low toxicity. Furthermore, PC' salts solutions were vastly used in lithium-ion batteries as electrolyte owing to its high ionic conductivity.[40-42] The organogel electrode thereby possessed good conductivity, excellent anti-freezing and solvent retention properties which had promising potentials in TENG construction.[43, 44] The organogel electrode was then sealed by two polydimethylsiloxane (PDMS) thin films to construct transparent TENG with high softness and flexibility, which was called Og-TENG in this work. With the high organicity of organogel, the compatibility between gels and PDMS was enhanced and further induced tougher adhesion in the interface than that of high polarity gels based TENG. Consequently, the Og-TENG could be folded, twisted and stretched without

delamination between electrode and elastomer layers. Og-TENG possessed wide working temperature range as it could tolerate -20℃ temperature environment as well as high temperature environment of 45℃. Moreover, the electric performance of Og-TENG is extraordinary, which reaches a high instantaneous power density of 4.03 W/m^2, exhibiting a higher power density than that of many recently reported gels electrode based TENGs. To the best of our knowledge, this was the first demonstration of organogel ionic conductor as electrode in transparent TENG. Og-TENG could be applied to harvest bio-mechanical energy for driving LEDs and electronic watch. Besides, the highly transparent Og-TENG had the potentials of electronic skin (e-skin) with good softness and flexibility, which was demonstrated in the detection of human gestures.

2. Results and discussion

2.1. Structure and properties of organogel and Og-TENG

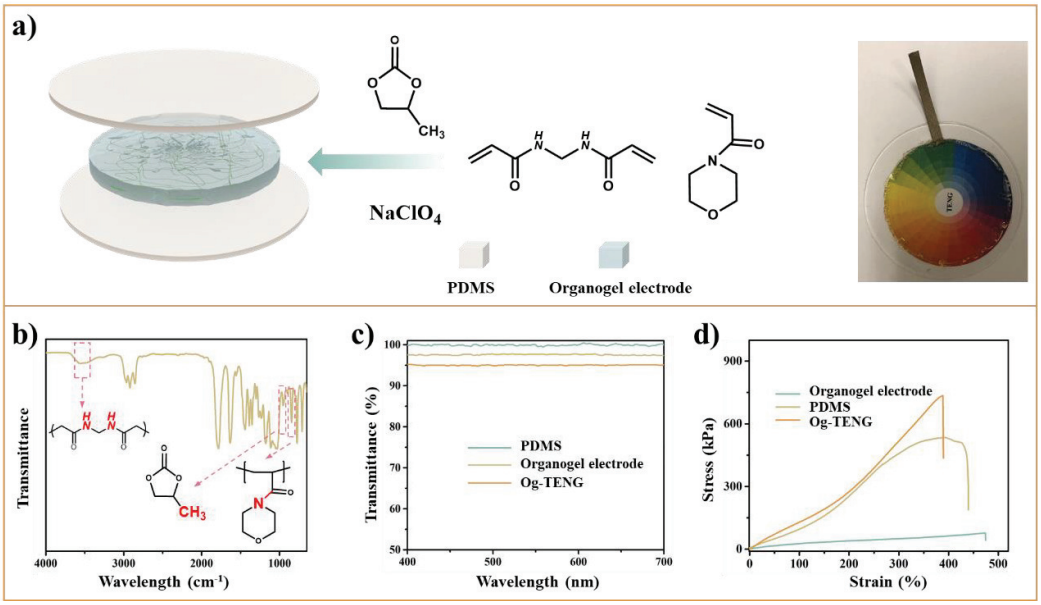

Figure 1. a) Sandwich-like architecture of Og-TENG, chemical synthesis route of organogel and digital photo of Og-TENG. b) FTIR spectrum of organogel. c) Transmittance of PDMS, organogel and Og-TENG. d) Uniaxial tensile test of PDMS, organogel and Og-TENG.

In this study, the organogel electrode was prepared from the photopolymerization and crosslinking of 4-acryloylmorpholine (ACMO), which formed the mainchain frame of gel. The solvent of gel was selected as sodium perchlorate PC solution for gel conductivity. Fig 1 shows chemical synthesis route of organogel and the chemical structure of organogel electrode was confirmed by Fourier transform infrared spectroscopy (FTIR). The absorption peak of 3565 cm^{-1} was attributed to the active hydrogen, which came from -NH of the crosslinking reagent in the gel. The spectrum of 2965~2857 cm^{-1} was assigned to -C−H stretching.[45] The characteristic vibration bands emerged at 1784 $cm^{-1}$and 1635 cm^{-1}, which were the stretching of ester -C=O and tertiary amide -C=O of PC and poly-ACMO. Another characteristic vibration band of mainchain poly-ACMO was the C-N stretching at the spectrum of 1272~1222 cm^{-1}. In terms of the PC solvent, the majority absorption was overlapped with poly-ACMO in mainchain such as $-CH_2$, -CO stretching. The characteristic vibration band of $-CH_3$

bending was observed at 1388 cm^{-1}, which showed the existence of PC. The -CO stretching of organogel was assigned to the spectrum of 1112~1029 cm^{-1}. From the results of FTIR, the gel preparation was proved to be successful. The conductivity of organogel was originated from the dissolved salts sodium perchlorate in PC. The resistivity of organogel electrode depended on the concentration of ionic sodium perchlorate, which exhibited a gradual decrease as the ion's concentration increased, i.e. from 59 KΩ·cm of 0.5 M, 53 KΩ·cm of 1.0 M, to 50 KΩ·cm of 1.5 M, as shown in Fig S1. The Og-TENG was schematically illustrated in Fig 1a, which was designed in a sandwich-like architecture. The organogel electrode was sealed by two PDMS films of 400 μm in thickness and the edge of TENG was sealed by PDMS to prevent solvent evaporation.[25] The sandwich-like architecture endowed Og-TENG with inherent capacitive behavior as an electrostatic system was formed, which could store more charges from the tribo-electrification.[25, 46-48] Consequently, the permittivity of Og-TENG was enhanced from 2.72 of pristine PDMS to 4.91 of Og-TENG, as shown in Fig S2. However, the concentration of sodium perchlorate had negligible influence on Og-TENG's permittivity as the ion concentration was above 0.5 M.

The organogel electrode is highly transparent and flexible as shown in Fig 1a, in which the concentration of sodium perchlorate was 0.5 M. The average transmittance of organogel electrode reached over 97% in visible region. The assembled Og-TENG thus possessed a good transmittance of 95% in visible region and the corresponding slight 2% drop in transparency was mainly resulted from light scattering at the interface of organogel electrode with PDMS.[20] The transmittance of organogel based TENG

achieved a high level which was similar with the excellent results from hydrogel based transparent TENG, such as polyacrylamide (PAAm)-LiCl hydrogel based TENG's 96.2%.[25] A comparison of performance between Og-TENG and other recently reported ionic conductors based TENGs was made and listed in Tab S1. The organogels with other thickness were also tested. As shown in Fig S3, even the thickness of organogel reached to 1.5 mm, the transmittance still maintained in a high level of over 92%, indicating high transparency of organogel. The mechanical properties of organogel and Og-TENG were evaluated by uniaxial tensile tests. As exhibited in Fig 1d, the organogel could be stretched to a maximum elongation of 474%, which possessed a higher stretchability than that of PDMS. The maximum elongation of Og-TENG reached to 387%, which was mainly decided by PDMS layer's breaking elongation. The sodium perchlorate concentration's influence on organogel was also measured, as shown in Fig S4. The elongation of organogel decreased with the gaining of salt concentration, which was gradually reduced from 537% at non salt to 327% at 1.5 M. In terms of the transmittance, all organogels possessed high transparency at different salt concentrations, as shown in Fig S4b.

2.2. Output performance and robustness of Og-TENG

The working mode of Og-TENG was in a single-electrode mode, in which a thin belt of conductive fabric was employed to connect the organogel to the ground. The work mechanism of TENG was based on tribo-electrification and electrostatic induction, which was shown in Fig 2a. Briefly, as triboelectrically positive materials such as conductive fabric were brought into contact with the Og-TENG's PDMS layer,

electrons were injected from triboelectrically positive materials to Og-TENG's PDMS film due to tribo-electrification between the two materials of opposite electron affinities. The same amount of charges with opposite polarities were thereby generated on the surfaces of PDMS and triboelectrically positive materials, the state Ⅰ. Once the contact of two materials was broken by separation, the unscreened negative charges on PDMS layer would impel the motion of positive ions Na^+ in the organogel, leading to the accumulation of positive charges Na^+ at the interface between PDMS and organogel. Meanwhile, the electrical double layer emerged at the interface between conductive fabric and organogel with the same amount of negative ions ClO_4^-. Consequently, electrons were driven from the connected conductive fabric belt to the ground for maintaining the electrical double layer and an electric signal was generated, the state Ⅱ. As the distance between the friction materials' surface was long enough, the positive charges on triboelectrically positive materials had limited equilibrium effect on the negative charges on PDMS. The unscreened negative charges were thereby increased which resulted in the increase of positive charges on the upper surface of organogel to achieve electrostatic equilibrium, the state Ⅲ. Once the Og-TENG's PDMS and triboelectrically positive materials approached back again, the whole process would be reversed and the electrons would be injected from ground to connect conductive fabric belt to equilibrate the positive charges in the conductive fabric and organogel's electrical double layer, the state Ⅳ. Hence, alternative current would be generated when contact-separation movement between the two friction materials was repeated by external force.

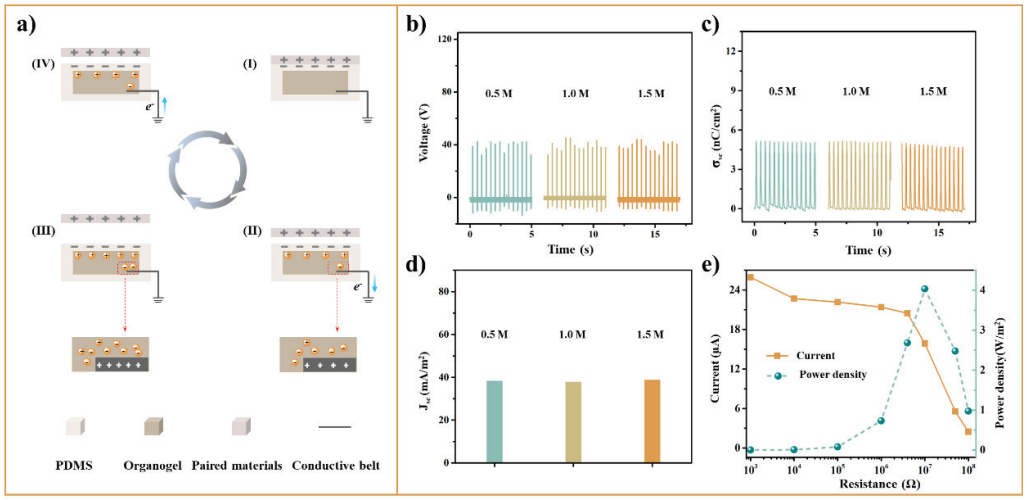

Figure 2. a) Working mechanism of Og-TENG. b) Output voltage of Og-TENG in different ion concentrations. c) Short-circuit charge transfer density (σ_{sc}) of Og-TENG in different ion concentrations. d) Short-circuit current density (J_{sc}) of Og-TENG in different salt concentrations. e) The instantaneous power density and output current of Og-TENG versus external load resistance where the salt concentration was 0.5 M.

The output performance of Og-TENG was measured in single-electrode with 1×2 cm^2 conductive fabric as triboelectrically positive material. The results are presented in Fig 2. It could be observed that an output signal of 44 V in voltage, 5.13 nC/cm^2 in short-circuit charge transfer density (σ_{sc}), and 38.3 mA/m^2 in short-circuit current density (J_{sc}) were generated when a periodical external force of around 2.8 Hz was applied to the Og-TENG at 0.5 M sodium perchlorate in organogel. The salt's concentration in organogel was varied to evaluate its influence on Og-TENG's output performance, which was also showed in Fig 2. As the salt concentration increased to 1.5 M, the electrode's conductivity was enhanced. However, compared to the large inner resistance of TENG (~ MΩ), the conductivity change of electrode had very little influence on the output current in circuit when the salt concentration was above 0.5 M. Besides, the capacitance of Og-TENG was generally not influenced by the concentration of salt, as shown in Fig S2. Hence, the Og-TENG rendered a steady

output performance, demonstrating salt concentration's negligible influence on output performance when the salt concentration was above 0.5 M. The sodium perchlorate in organogel was fixed at 0.5 M in further study. Other salt concentrations' performance was also investigated and the output voltage showed obvious declining when the salt concentrations was reduced to 0.1 M, as shown in Fig S5. A series of resistances of different values (10^3~10^8 Ω) were then directly connected to the TENG for testing its output performance as a power source. Fig 2e showed that the output current of Og-TENG decreased gradually with the gaining external resistance values. Meanwhile, the power density reached its peak of 4.03 W/m^2 at external resistance of 10^7 Ω. This power density was much higher than many recently reported gel ionic conductors based TENGs, demonstrating that the organogel was an excellent candidate as a gel ionic conductor in transparent TENGs. The details of power density comparison were presented in Tab S1.

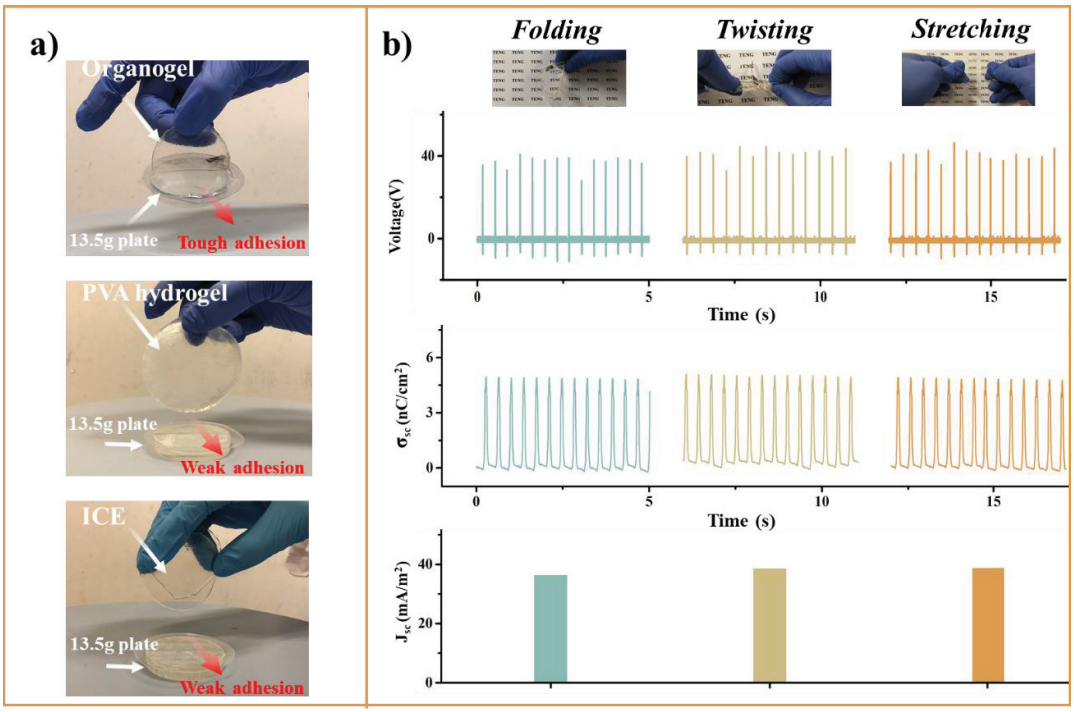

Figure 3. a) Electrode-PDMS's interface adhesion comparison between organogel, hydrogel and ICE by lifting up. b) Output voltage, σ_{sc} and J_{sc} of Og-TENG after 100 cyclic times of different kinds of deformation, respectively.

Up to now, hydrogels or ionogel such as polyvinyl alcohol (PVA) or PAAm hydrogel were widely used as conductive gel to fabricate flexible and transparent TENGs. However, due to high polarity of such gels, the adhesion between gels and low polarity triboelectric elastomer interface was weak, which usually reduced gel based TENG's mechanical reliability.[37, 38] To address the problem, some works employed chemical bonding method to achieve tough bonding between high polarity gel and low polarity elastomer.[37-39] However, the chemical process was complex and the TENG's transparency was sacrificed. In this work, the swelling solvent used in organogel was selected as organic propylene carbonate, which was low polarity solvent as compared to water. The bonding effectiveness between gel and low polarity PDMS was thereby boosted. Polymer ion-conducting elastomer conductors such as poly(butyl

acrylate) elastomer were also used in electrode of TENG as the high thermal stability.[35] However, elastomer usually has less stickiness than gel which made it hard to obtain tough interface. To demonstrate the strong adhesion between organogel and PDMS, a PMMA plate of 13.5 g was attached to the bottom PDMS film of Og-TENG, and the interface between gel and bottom PDMS layer was carefully peeled off. The free end of the gel with upper PDMS layer was lifted up and the PMMA plate could be steadily held, as shown in Fig 3a. For comparison, PVA fabricated hydrogel and a ion-conducting elastomer electrode (ICE) were used to replace the role of organogel in TENG. However, the interface between PVA hydrogel or ICE and PDMS was easily broken when it was lifted up like Og-TENG, which could be seen in Fig 3a and SI video-1. The excellent adhesion between organogel and PDMS layer endowed Og-TENG with good mechanical reliability, which made it a robust TENG for different deformations. As exhibited in Fig 3b, Og-TENG was folded, twisted and stretched by hand for 100 cyclic times, respectively. Delamination was not observed and the TENG's output performance maintained its initial value.

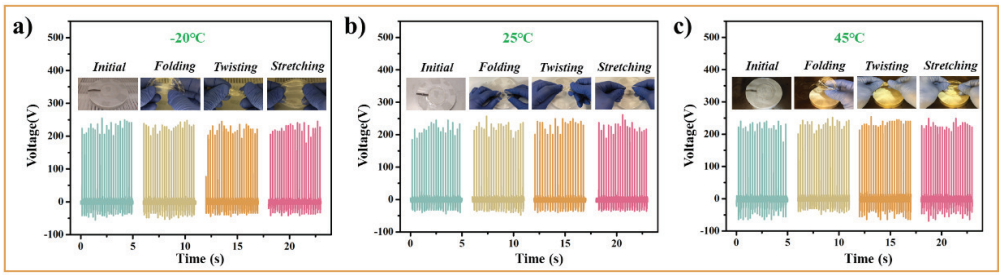

Figure 4. Output voltages of Og-TENG after different kinds of deformation at different working temperatures of a) -20 ℃, b) 25 ℃ and c) 45 ℃. The working mode was single-electrode with hand tapping.

PC used in organogel electrode possesses a freezing point of -49 ℃ and a boiling point of 242 ℃, which exhibits a much higher temperature range than that of water used

in hydrogel electrode. The major concern of hydrogel based TENG was that it would be embrittlement and easily broken when it was used in low temperature environment of below 0 ℃.[32] Herein, the wide temperature range of organic solvent endowed the organogel and Og-TENG with a large applicable temperature range over hydrogel based TENG. Ogranogel and assembled TENG thereby could tolerate lower temperature owing to the low freezing point of solvent in organogel electrode. As shown in Fig S6a, after 5 h in -20 ℃ environment, organogel exhibited its initial shape while the PVA hydrogel became brittle and easily broken. To further demonstrate its resistance to low temperature, Og-TENG was stored at -20 ℃ environment for 5 days. Encouragingly, as shown in SI video-2, Og-TENG still maintained its initial flexibility and could be twisted and stretched, indicating no embrittlement of the TENG at such low temperature. Delamination between electrode layer and PDMS layer was also not found, exhibiting that tough interface bonding was still effective at -20 ℃ environment. The output performance at such low temperature was further evaluated to demonstrate the low temperature tolerance of Og-TENG. Hand tapping with glove was conducted in such test, which was also in single-electrode mode. As exhibited in Fig 4a and SI video-3, a wide output voltage was observed when the TENG was tapped by hand, which could reach over 200 V even after the TENG was suffered different deformations. Moreover, the output voltage did not show obvious declining as compared to that in 25 ℃ environment, which further proved that the TENG possessed high tolerance to low temperature and excellent electric reliability and mechanical robustness. The output performances of TENG after different kinds of deformation at

high temperature of 45 ℃ were also measured for demonstration of the tolerance of high temperature and they showed similar results to that of -20 ℃ and 25 ℃. These experimental data illustrated the Og-TENG's applicability and reliability in daily temperature range, which could be applied in harsh environment for energy harvesting.

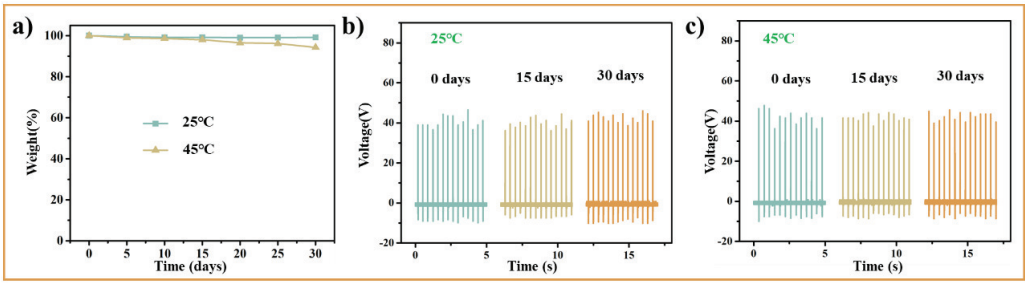

Figure 5. a) Weight variation of Og-TENG in 30 days at different environment temperatures. b) Og-TENG's output voltages after 0 days, 15 days and 30 days at 25 ℃ storing environment temperature, respectively. c) Og-TENG's output voltages after 0 days, 15 days and 30 days at 45 ℃ storing environment temperature, respectively.

The dehydration along with time was the another major concern in the application of gel based TENG, as the solvent in gel would be volatilized under hot temperature and thus reduce gel's mechanical elasticity.[25] Owing to the high boiling point and low vapor pressure of PC, the organogel electrode possessed high resistance to high temperature and could tolerate high temperature of 80 ℃ for 1 h with negligible change in appearance, which was presented in Fig S6b. Thermogravimetric analysis curves of organogel and hydrogel provided more information about thermal stability, as shown in Fig S7. It is notable that only 6.7% weight loss in organogel appeared when it was heated to 150 ℃. However, 85% weight loss was observed in PVA hydrogel which indicated that the water solvent was evaporated totally. The excellent thermal stability of organogel originates from the high boiling point of its swelling solvent and the results implied that the organogel had promising potentials in anti-dehydration. To further

evaluate the dehydration of Og-TENG, the weight variation of the TENG in hot and dry 45 ℃ oven environment as well as 25 ℃ indoor environment were measured and plotted in Fig 5a. As expected, the weight of Og-TENG exhibited a slight change after the TENG was stored for 30 days at 45 ℃ oven environment, which kept 94% of initial weight. The mechanical elasticity of Og-TENG was thereby maintained which could be folded or twisted. Meanwhile, the output performance of Og-TENG was maintained. The output voltages of Og-TENG in single-electrode mode at different storing time were measured by periodical applied force on the TENG, which were 48 V at 10 days, 44 V at 15 days and 46 V at 30 days and no notable change was observed as compared to initial output voltage, as shown in Fig 5. Under the 25 ℃ indoor environment, the weight of Og-TENG as well as output voltage exhibited negligible change as compared to that of TENG stored for 30 days. In general, these excellent anti-dehydration properties of the Og-TENG made the TENG a robust device, which could be applicable to harsh temperature environment.

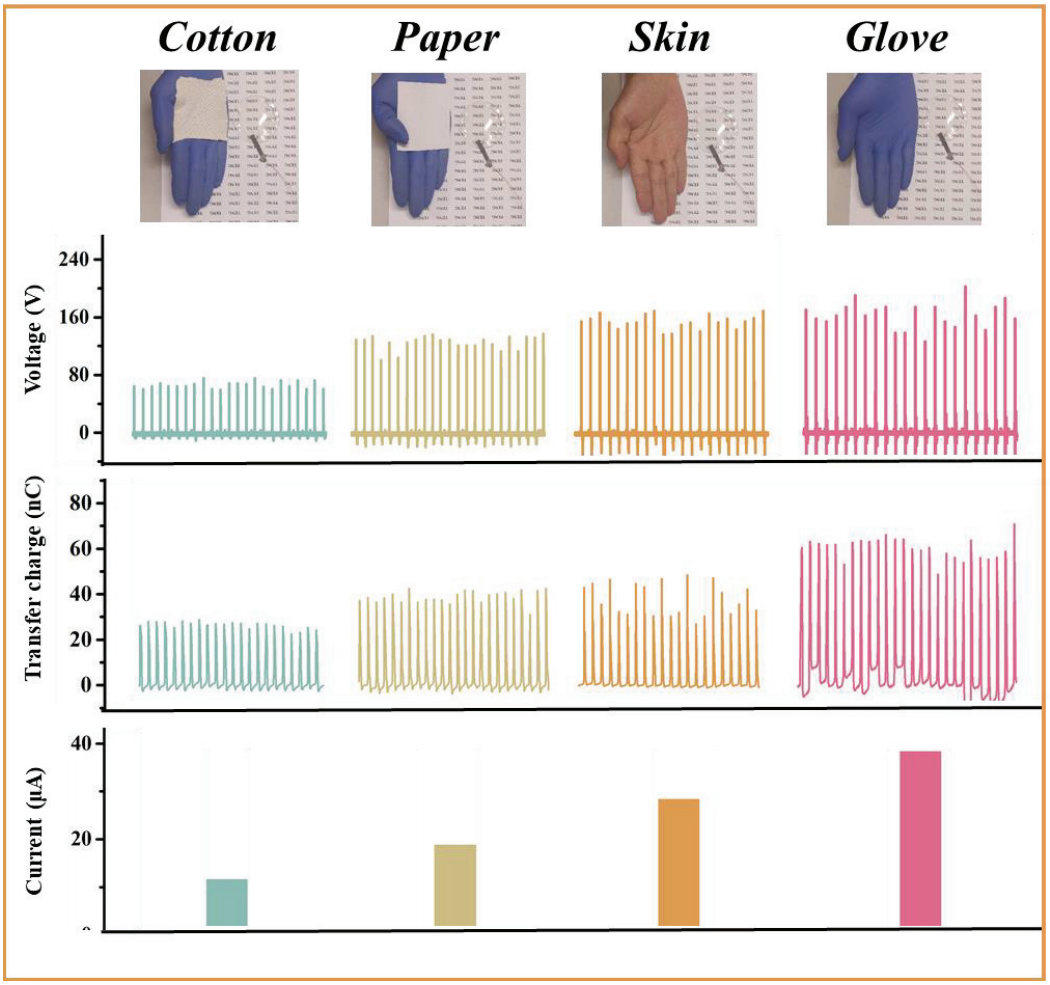

Figure 6. Output amplitude of Og-TENG which is paired with different materials of cotton, paper, skin and glove. The working mode was single-electrode with hand tapping.

The output amplitude of TENG strongly depended on the friction pair of different electron affinities in triboelectrification. A series of materials were utilized as triboelectrically positive materials for the demonstration of Og-TENG's ability of power generating in real application. The working mode of Og-TENG was single-electrode with hand tapping on a sample of an effective area of 44 mm in diameter. The output amplitude of Og-TENG was shown in Fig 6, where the hand with different materials was brought into contact and separation with the TENG. Among these materials, nitrile glove possessed highest output performance with over 200 V in output

voltage, 71 nC in charge transfer, and 43 μA in short-circuit current. Human skin also showed a high output performance of 169 V in output voltage, 49 nC in charge transfer, and 31 μA in short-circuit current, which was only inferior to that of nitrile glove. As for the paper and cotton fabric, the output performances were lower than that of skin. The two-electrode working mode of these materials was also evaluated and conductive fabric was used as back electrode in the working mode, which were shown in Fig S8. The output performances were higher than their single-electrode working mode, in which nitrile glove paired TENG could reach over 300 V in output voltage. Besides, their order of output performance in single-electrode or two-electrode working mode were nitrile glove > human skin > paper > cotton. The results were coincident with the reported tribo-series because of the materials difference in ability of losing electrons.[49] In addition, the organogel electrode can also be applied to other polymers, such as FEP, PTFE. The output performance of such TENGs was shown in Fig S9. The output voltages reached to 163 V for FEP and 197 V for PTFE, indicating the organogel electrode could be directly applied to other friction materials. Generally, Og-TENG was applicable with different kinds of materials for energy harvesting.

To further demonstrate the reliability of Og-TENG, the output voltages of Og-TENG as well as digital photos in different stretched states were tested and presented in Fig S10. The Og-TENG was tailored into rectangle for facile illustration of stretched state. As the stretchable Og-TENG was hard to be fixed in the plate of our test device, the output voltages of stretchable Og-TENG were obtained from tapping with forefinger. As shown in Fig S10, the Og-TENG could be stretched to more than 3-fold of its initial

length (λ≈3). However, the output voltage decreased with the Og-TENG's elongation. In such test method, the contact area was intersection between forefinger and Og-TENG, which was decided by the fixed forefinger's width and the changed Og-TENG's width. When Og-TENG was stretched in lengthwise direction, its cross section exhibited a shrinkage and the Og-TENG's width was thereby reduced. The resulting less contact area further induced the decrease of output voltage. When the stretching force was released, Og-TENG recovered it original length (λ=1) with recovered output voltage. The results further illustrated that the Og-TENG could work in stretched states which was reliable in different stretched states.

2.3. Og-TENG's performance as power source and sensor

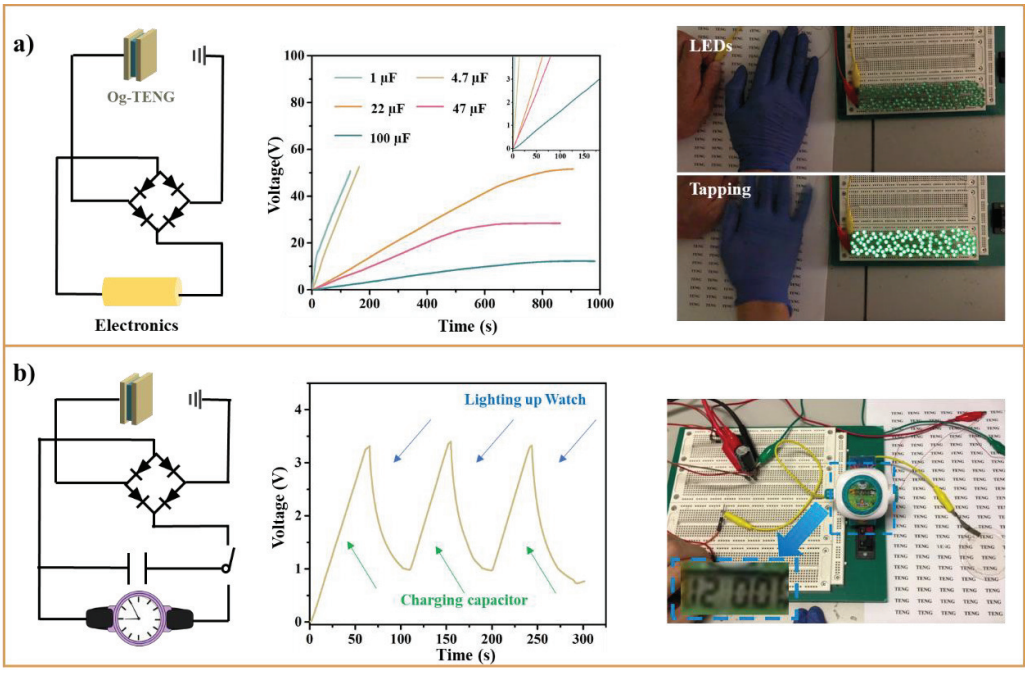

Figure 7. The ability Og-TENG as a power source. a) The circuit of powering electronics, capacitor charging curve (voltage versus time, the insertion figure was the charging process under 3.0 V), and the lighting of 116 green LEDs. b) The circuit of powering electric watch, capacitor charging curve (voltage *versus* time) and the photo of circuit and electric watch

The Og-TENG with high output performance could be applied to harvest bio-mechanical energy which could further power many electronics. As a demonstration, 116 green LEDs were connected to the TENG in series circuit. With the nitrile glove equipped hand tapping on the Og-TENG at frequency of around 4 Hz, output electricity generated from the TENG was adjusted by a rectifier bridge. As exhibited in Fig 7 and SI video-4, the electric output could light up the 116 green LEDs with good brightness. The TENG's potential of capacitor charging was presented in Fig 7a, which was plotted in voltage *versus* time by a series capacitor of different values. It could be observed that voltage of capacitor rapidly increased when hand periodically tapped on the TENG. The voltages of 22 μF, 47 μF and 100 μF capacitors reached to 52 V, 29 V and 12 V respectively when the voltages were steady. For 1 μF and 4.7 μF capacitors, considering their safe voltages are 50 V, the charging process was stopped at around 50 V. The charging rates were then calculated by the used time for the voltage of charged capacitor reaching 3.0 V, which were 822 mV/s@1μF, 278 mV/s@4.7μF, 61 mV/s@22μF, 49 mV/s@47μF and 16 mV/s@100μF respectively. The capacitor charging rate in this work was much higher than that of recently reported gel electrode based TENGs, which further proved Og-TENG's potential as a power source, as shown in Tab S1.

The electricity stored in capacitor thereby could be used to power some electronics. In a demonstrative experiment, an electric watch was connected to the TENG with 22 μF capacitor and the circuit was shown in Fig 7b. The capacitor was charged by Og-TENG with hand tapping at first and the voltage of capacitor achieved 3.3 V within 60 seconds. The circuit was subsequently switched to connect the watch. The watch was

powered to work normally by the electricity in the capacitor. The working time of watch reached over 40 seconds until the voltage of capacitor decreased to around 1 V. The circuit was then switched back to connect the Og-TENG for recharging of the capacitor. After around 40 seconds of hand tapping on the generator, the voltage of capacitor went back to 3.3 V. The powering process of watch could be repeated periodically, as shown in Fig 7b.

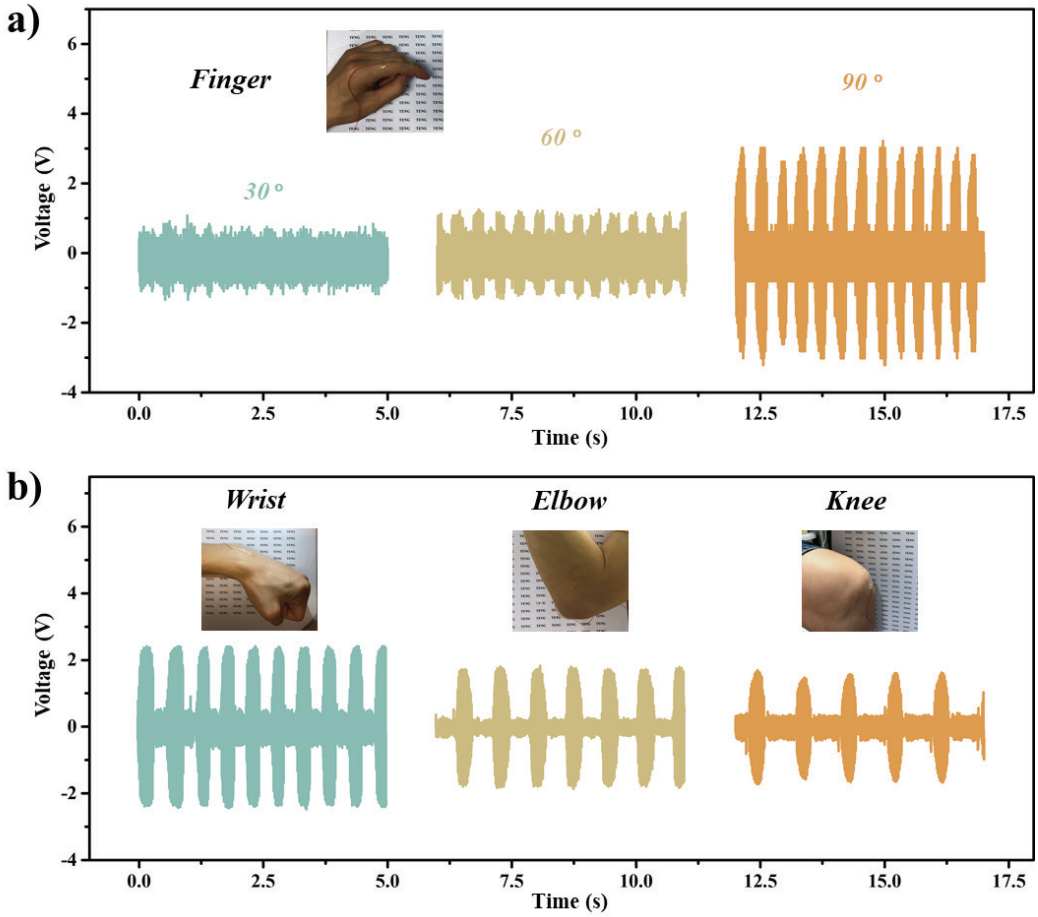

Figure 8. Output signals generated from Og-TENG, by a) finger bending at different bending angles, b) wrist bending, elbow bending and knee bending.

The high transparency, flexibility as well as high output performance endowed Og-TENG with great potential in e-skin applications which required high flexibility

and sensitivity in responding to externally stimulation.[50, 51] Og-TENG was tailored into a belt of 1×5 cm^2 for detecting human moving gestures, as shown in Fig 8. The Og-TENG's surface PDMS was comfortable to human skin and the end of Og-TENG were fixed on the moving parts of human body by double-sided adhesive. The output signal was detected by an oscilloscope which was connected to the Og-TENG through a Cu wire. As shown in Fig 8, output signal could be clearly observed in the bending motions of human body parts such as finger, wrist, elbow and knee. In detail, when the Og-TENG was employed to detect the finger bending, the output voltages were varied as the finger bending angle was varied from 30°, 60° to 90°. The wrist, elbow and knee bending could also be detected by the Og-TENG. As a self-powered device, the output signal was generated from Og-TENG, which had no requirement of additional energy supply or storage device. Furthermore, the gesture detection device was transparent and the skin behind the device could be clearly observed in various movement. These results manifested that Og-TENG had great potentials in the e-skin applications.

3. Conclusion

In summary, an organogel electrode, consisted of Poly(4-acryloylmorpholine) frame and low polarity propylene carbonate swelling solvent, was prepared for constructing a new kind of organogel ionic electrode based TENG, Og-TENG, in this work. The Og-TENG was constructed from the package of organogel electrode by two thin PDMS films, which possessed a high transparency of 95%, stretchability of 387% and daily working temperature range of -20℃- 45℃. Owing to the higher compatibility

between the organogel electrode and PDMS elastomer than that of high polarity gel electrode, the interface adhesion was boosted, which resulted in tough bonding between the gel and elastomer. Consequently, Og-TENG exhibited outstanding electric reliability and mechanical robustness in energy harvesting, which could be folded, twisted and stretched without delamination in daily working temperature range (-20℃-45℃). The electric performance of Og-TENG was extraordinary, reaching a high instantaneous power density of 4.03 W/m^2. The transparent Og-TENG was further employed to harvest biomechanical energies and detect human moving gestures, demonstrating its promising potential in wearable electronics, e-skin, etc. This work demonstrated that organogel electrode has a great potential in TENG constructions and more organogels are worthy to be explored as the vast choices for making transparent, stretchable and reliable TENGs of high power density for energy harvesting.

4. Experiment section

Materials and Characterization

Propylene carbonate (PC) and sodium perchlorate were bought from Alfa Aesar and PDMS (Sylgard 184) was the product of Dow Corning. 4-acryloylmorpholine (ACMO, monomer), N,N'-Methylenebisacrylamide (MBA, cross-linker), Polyvinyl alcohol(Mw~205,000), Butyl acrylate (BA), poly-ethyleneg-lycol diacrylate (PEGDA Mw~1,000), bis(trifluoromethane sulfonimide) (LiTFSI) and 1-hydroxycyclohexyl phenyl ketone (photoinitiator 184) were obtained from Dieckmann company. Cu/Ni

coated fabric which was purchased from 3 M Corp, was applied as conductive fabric. All reagents were used as received without further purification.

The FTIR of gel was performed on PerkinElmer. Inc, Spectrum100. The transmittance of samples was measured by Hitachi UH5300. The periodically external force for evaluating TENG's out performance was obtained from Button/key durability life test machine, ZX-A03, Zhongxingda Shenzhen. The resistivity of organogel electrode was measured by Four-probe tester STST-2258A, Suzhou Jingge Electronic Co. LTD. The dielectric constant of the TENG was calculated from its capacitance. $C = \varepsilon_0 * S\frac{\varepsilon_r}{d}$ and the capacitance was acquired from LCR-6300,300kHz, GW Instek. The uniaxial tensile test was obtained from instron5900. Thermogravimetric analysis curve was obtained from Mettler Toledo TGA/DSC1 system with heating rate of 10 ℃/min in air. The output voltage was recorded by oscilloscope of Keysight Infiniivision DSOX3024T. Keithley 6514 system electrometer of Tektronix, Inc was used to measure the TENG's output current and transfer charge.

Preparation of PDMS film

The PDMS pre-polymer and curing agent were mixed in mass ratio of 10:1 to prepare the PDMS pre-cured solution. The PDMS pre-cured solution was then cast on plastic dish for designed thickness of around 400 μm. After degassing of bubbles, the PDMS pre-cured solution was placed in oven at 80 ℃ for 1 h. The cured PDMS thus was obtained by peeling off from dish when the film was cooled to room temperature.

Preparation of PACMO-$NaClO_4$ organogel and Og-TENG

The organogel was prepared from the photocrosslinking of ACMO, which was a modification of reported work.[42, 44] In detail, ACMO and sodium perchlorate's PC solution were mixed at the volume ratio of 50:50. Cross-linker MBA and photoinitiator 184 were then added to the mixed solution at molar ratio of 0.1% and 1% respectively. The pre-organogel solution was thus prepared for use.

In a transparent flat PMMA substrate, PDMS film was used to cover its surface as the lower surface of chemical mold. A silicone circular ring of 500 μm thickness was placed on it and applied as supporter to form mold. Another transparent flat PMMA substrate of 44 mm in diameter with PDMS film covering was used as the upper surface of mold. The pre-organogel solution was then injected into the mold by syringe. After that, the mold was irradiated by 365 nm ultraviolet light of 75 W for 40 mins to cure the solution. The PACMO-$NaClO_4$ organogel was obtained. The PMMA substrate and silicone circular ring were taken away and the PMDS-Organogel-PDMS sandwich architecture was obtained. A thin belt of conductive fabric was carefully attached to the organogel. Finally, the edge of sandwich architecture was poured by PDMS solution and was placed in 80 ℃ oven for 1 h to seal the organogel. The Og-TENG was thus obtained.

Preparation of PVA hydrogel

PVA was dissolved in boiling water at mass ratio of 15% to form a viscous and clear solution. The solution was cast on a clean dish and stored in -20 ℃ environment for 8 h with subsequent placement in air to melt the mixture. The freezing and melting process were repeated for twice cycles and the PVA hydrogel was formed.

Preparation of ICE hydrogel

Butyl acrylate monomer was used to dissolve LiTFSI at 0.5 M concentration. After that, PEGDA crosslinker and photoinitiator 184 were then added to the mixed solution at mass ratio of 0.1% and 1% respectively. The ion-conducting elastomer electrode (ICE) was fabricated by a free radical photopolymerization of with 365 nm ultraviolet light of 75 W for 120 mins.[35]

Acknowledgements

The authors acknowledge The Hong Kong Polytechnic University (G-YBV2) for funding supports of this work.

References:

[1] F.R. Fan, W. Tang, Z.L. Wang, Advanced Materials, 28 (2016) 4283-4305.
[2] X. Cao, Y. Jie, N. Wang, Z.L. Wang, Advanced Energy Materials, 6 (2016).
[3] K. Parida, V. Kumar, W. Jiangxin, V. Bhavanasi, R. Bendi, P.S. Lee, Adv Mater, 29 (2017).
[4] L. Zhou, D. Liu, J. Wang, Z.L. Wang, Friction, 8 (2020) 481-506.
[5] J. Wang, S. Li, F. Yi, Y. Zi, J. Lin, X. Wang, Y. Xu, Z.L. Wang, Nat Commun, 7 (2016) 12744.
[6] Z.L. Wang, T. Jiang, L. Xu, Nano Energy, 39 (2017) 9-23.
[7] J. Liu, L. Gu, N. Cui, Q. Xu, Y. Qin, R. Yang, Research, 2019 (2019) 1-13.
[8] Q. Zhou, J.G. Park, K.N. Kim, A.K. Thokchom, J. Bae, J.M. Baik, T. Kim, Nano Energy, 48 (2018) 471-480.
[9] F.R. Fan, L. Lin, G. Zhu, W. Wu, R. Zhang, Z.L. Wang, Nano Lett, 12 (2012) 3109-3114.
[10] H. Chu, H. Jang, Y. Lee, Y. Chae, J.-H. Ahn, Nano Energy, 27 (2016) 298-305.
[11] Q. Shi, T. He, C. Lee, Nano Energy, 57 (2019) 851-871.
[12] K. Dong, Y.C. Wang, J. Deng, Y. Dai, S.L. Zhang, H. Zou, B. Gu, B. Sun, Z.L. Wang, ACS Nano, 11 (2017) 9490-9499.
[13] J. Gong, B. Xu, X. Guan, Y. Chen, S. Li, J. Feng, Nano Energy, 58 (2019) 365-374.
[14] T. Jing, B. Xu, Y. Yang, Nano Energy, 74 (2020).

[15] L. Zhang, Y. Liao, Y.C. Wang, S. Zhang, W. Yang, X. Pan, Z.L. Wang, Advanced Functional Materials, (2020).
[16] Z. Wang, Z. Ruan, W.S. Ng, H. Li, Z. Tang, Z. Liu, Y. Wang, H. Hu, C. Zhi, Small Methods, 2 (2018).
[17] K. Dong, X. Peng, J. An, A.C. Wang, J. Luo, B. Sun, J. Wang, Z.L. Wang, Nat Commun, 11 (2020) 2868.
[18] X. Peng, K. Dong, C. Ye, Y. Jiang, S. Zhai, R. Cheng, D. Liu, X. Gao, J. Wang, Z.L. Wang, Science Advances, 6 (2020) eaba9624.
[19] X. Guan, B. Xu, J. Gong, Nano Energy, 70 (2020).
[20] L. Wang, W.A. Daoud, Advanced Energy Materials, (2018).
[21] A. Yu, Y. Zhu, W. Wang, J. Zhai, Advanced Functional Materials, (2019).
[22] B. Chen, W. Tang, T. Jiang, L. Zhu, X. Chen, C. He, L. Xu, H. Guo, P. Lin, D. Li, J. Shao, Z.L. Wang, Nano Energy, 45 (2018) 380-389.
[23] J. Gong, B. Xu, X. Tao, ACS Appl Mater Interfaces, 9 (2017) 4988-4997.
[24] J. Chen, H. Guo, C. Hu, Z.L. Wang, Advanced Energy Materials, 10 (2020).
[25] X. Pu, M. Liu, X. Chen, J. Sun, C. Du, Y. Zhang, J. Zhai, W. Hu, Z.L. Wang, Sci Adv, 3 (2017) e1700015.
[26] F.-R. Fan, Z.-Q. Tian, Z. Lin Wang, Nano Energy, 1 (2012) 328-334.
[27] C. Wu, A.C. Wang, W. Ding, H. Guo, Z.L. Wang, Advanced Energy Materials, 9 (2019).
[28] X. Wang, Y. Zhang, X. Zhang, Z. Huo, X. Li, M. Que, Z. Peng, H. Wang, C. Pan, Adv Mater, 30 (2018) e1706738.
[29] J. Wang, C. Wu, Y. Dai, Z. Zhao, A. Wang, T. Zhang, Z.L. Wang, Nat Commun, 8 (2017) 88.
[30] Y.-T. Jao, P.-K. Yang, C.-M. Chiu, Y.-J. Lin, S.-W. Chen, D. Choi, Z.-H. Lin, Nano Energy, 50 (2018) 513-520.
[31] S. Niu, S. Wang, L. Lin, Y. Liu, Y.S. Zhou, Y. Hu, Z.L. Wang, Energy & Environmental Science, 6 (2013).
[32] L. Sun, S. Chen, Y. Guo, J. Song, L. Zhang, L. Xiao, Q. Guan, Z. You, Nano Energy, 63 (2019).
[33] G. Zhao, Y. Zhang, N. Shi, Z. Liu, X. Zhang, M. Wu, C. Pan, H. Liu, L. Li, Z.L. Wang, Nano Energy, 59 (2019) 302-310.
[34] Y. Jian, B. Wu, X. Le, Y. Liang, Y. Zhang, D. Zhang, L. Zhang, W. Lu, J. Zhang, T. Chen, Research (Wash D C), 2019 (2019) 2384347.
[35] P. Zhang, Y. Chen, Z.H. Guo, W. Guo, X. Pu, Z.L. Wang, Advanced Functional Materials, (2020).
[36] P. Lv, L. Shi, C. Fan, Y. Gao, A. Yang, X. Wang, S. Ding, M. Rong, ACS Appl Mater Interfaces, 12 (2020) 15012-15022.
[37] T. Liu, M. Liu, S. Dou, J. Sun, Z. Cong, C. Jiang, C. Du, X. Pu, W. Hu, Z.L. Wang, ACS Nano, 12 (2018) 2818-2826.
[38] H. Yuk, T. Zhang, G.A. Parada, X. Liu, X. Zhao, Nat Commun, 7 (2016) 12028.
[39] X. Jing, H. Li, H.-Y. Mi, P.-Y. Feng, X. Tao, Y. Liu, C. Liu, C. Shen, Journal of Materials Chemistry C, (2020).

[40] R. Payne, I.E. Theodorou, The Journal of Physical Chemistry, 76 (1972) 2892-2900.
[41] N. von Aspern, G.V. Roschenthaler, M. Winter, I. Cekic-Laskovic, Angew Chem Int Ed Engl, (2019).
[42] L. Shi, R. Yang, S. Lu, K. Jia, C. Xiao, T. Lu, T. Wang, W. Wei, H. Tan, S. Ding, NPG Asia Materials, 10 (2018) 821-826.
[43] J. Song, S. Chen, L. Sun, Y. Guo, L. Zhang, S. Wang, H. Xuan, Q. Guan, Z. You, Adv Mater, 32 (2020) e1906994.
[44] Y. Gao, L. Shi, S. Lu, T. Zhu, X. Da, Y. Li, H. Bu, G. Gao, S. Ding, Chemistry of Materials, 31 (2019) 3257-3264.
[45] F. Xu, H. Li, Y.L. Luo, W. Tang, ACS Appl Mater Interfaces, 9 (2017) 5181-5192.
[46] M.D. Bartlett, A. Fassler, N. Kazem, E.J. Markvicka, P. Mandal, C. Majidi, Adv Mater, 28 (2016) 3726-3731.
[47] Z.M. Dang, J.K. Yuan, S.H. Yao, R.J. Liao, Adv Mater, 25 (2013) 6334-6365.
[48] H. Kang, H.T. Kim, H.J. Woo, H. Kim, D.H. Kim, S. Lee, S. Kim, Y.J. Song, S.-W. Kim, J.H. Cho, Nano Energy, 58 (2019) 227-233.
[49] H. Zou, Y. Zhang, L. Guo, P. Wang, X. He, G. Dai, H. Zheng, C. Chen, A.C. Wang, C. Xu, Z.L. Wang, Nat Commun, 10 (2019) 1427.
[50] P.S. Das, A. Chhetry, P. Maharjan, M.S. Rasel, J.Y. Park, Nano Research, 12 (2019) 1789-1795.
[51] K. Dong, Z. Wu, J. Deng, A.C. Wang, H. Zou, C. Chen, D. Hu, B. Gu, B. Sun, Z.L. Wang, Adv Mater, 30 (2018) e1804944.